Available online at www.sciencedirect.com
SCIENCE DIRECT
Nuclear Instruments and Methods in Physics Research A 563 (2006) 368–376
NUCLEAR INSTRUMENTS & METHODS IN PHYSICS RESEARCH Section A
www.elsevier.com/locate/nima

Status report on silicon photomultiplier development and its applications ☆

B. Dolgoshein[a,*], V. Balagura[b], P. Buzhan[a], M. Danilov[b], L. Filatov[d], E. Garutti[c], M. Groll[e], A. Ilyin[a], V. Kantserov[a], V. Kaplin[a], A. Karakash[a], F. Kayumov[a], S. Klemin[d], V. Korbel[c], H. Meyer[c], R. Mizuk[b], V. Morgunov[b], E. Novikov[b], P. Pakhlov[b], E. Popova[a], V. Rusinov[b], F. Sefkow[c], E. Tarkovsky[b], I. Tikhomirov[b], Calice/SiPM Collaboration

[a] *Moscow Engineering and Physics Institute, Kashirskoe shosse 31, 115409, Moscow, Russia*
[b] *Institute of Theoretical and Experimental Physics, B. Cheremushkinskaya 25, Moscow, Russia*
[c] *DESY, Notkestrasse 85, 22607 Hamburg, Germany*
[d] *State Unitary Science & Production Enterprise (PULSAR), Okruzhnoy proezd 27, Moscow, Russia*
[e] *University of Hamburg, Germany*

Available online 24 March 2006

Abstract

The state of art of the Silicon Photomultipliers (SiPM's)—their features, possibilities and applications—is given. The significant progress of this novel technique of photo detection is described and discussed.

Keywords: Silicon Photomultiplier; Hadron calorimeter; Wavelength shifter; Scintillation detector; Time-of-flight measurements

1. Silicon Photomultiplier description and performance

1.1. Principle of operation

The Silicon Photomultiplier (SiPM) is a novel semiconductor photodetector operated in limited Geiger mode [1–7]. It reaches an intrinsic gain for single photoelectrons at the level of 10^6, comparable to that of vacuum phototubes (PMTs) and considerably higher than that of avalanche photo-diodes (APDs) operated in proportional mode. The relatively inexpensive device consists of an array of small (~20–30 μm) independent pixels arranged on a common substrate to form a macroscopic unit of 1–3 mm size, with 500–4000 pixels/mm^2. Each pixel is operated with a bias voltage V_{bias} a few volts above breakdown voltage $V_{\text{breakdown}}$. In this mode a photoelectron created in the silicon and reaching the high field region by diffusion or drift initiates a Geiger discharge confined to that pixel. The discharge is quenched by limiting the current to about 10 μA with a small polysilicon resistor in each pixel. The independently operating pixels are connected to the same readout line; therefore the combined output signal corresponds to the sum of all fired pixels, which is a measure of the light flux.

1.2. Photon detection efficiency by SiPM

Like other silicon-based photodetectors, the SiPM has high-quantum efficiency (QE) close to 100% for optical photons. However, the overall photon detection efficiency (PDE) for present-state SiPMs is smaller due to several additional contributions apart from the QE:

- geometrical efficiency $\varepsilon_{\text{geom}}$ (the fraction of sensitive area on the detector surface),
- probability for a photo-electron to initiate a Geiger discharge,
- recovery time of the pixel.

☆ Presented by B. Dolgoshein at TRD2005 conference, Bari, Italy, 7–10 September 2005.

*Corresponding author. Tel./fax: +7 095 3247105.
E-mail address: boris@mail.cern.ch (B. Dolgoshein).

0168-9002/$ - see front matter
doi:10.1016/j.nima.2006.02.193

The spectral behavior of the PDE is driven in general by the photon absorption length in Si (from 0.01 to few μm for wavelengths $300\,\text{nm} < \lambda < 700\,\text{nm}$). Fig. 1 shows the PDE for present-state SiPMs in comparison with the typical QE of APDs and PMTs. The SiPM PDE is at the level of the PMT QE for blue light and larger in the yellow-red region, which is important for readout of scintillators via wavelength shifter (WLS) fibers.

The probability for a Geiger discharge (typically 60–70%) and thus the overall SiPM PDE depends on the bias voltage through the ionization coefficient.

1.3. Gain of SiPM

The Geiger signal from one pixel is determined by the charge $Q_{\text{pixel}} = C_{\text{pixel}} \cdot \Delta V$ accumulated in the pixel capacitance C_{pixel}. The overvoltage $\Delta V = V_{\text{bias}} - V_{\text{breackdown}}$ .is of order of a few volts and C_{pixel} is typically 50 fF; so Q_{pixel} is of the order of 150 fC or 10^6 electrons. The single pixel gain increases linearly with overvoltage, in contrast to the exponential voltage dependence of the gain of APDs.

One pixel signal on 50 Ω load corresponds to a pulse amplitude of ~1 mV (for a typical 10–20 ns pulse) and can be transmitted to the front end electronics over several meters distance without requiring a preamplifier near the photodetector.

1.4. Photon counting capability

A SiPM pulse height spectrum generated by the dark rate is shown in Fig. 2. One can see an excellent single photoelectron (single pixel) resolution, which is a consequence of

- good pixel to pixel gain uniformity,
- negligible contribution of electronics noise,

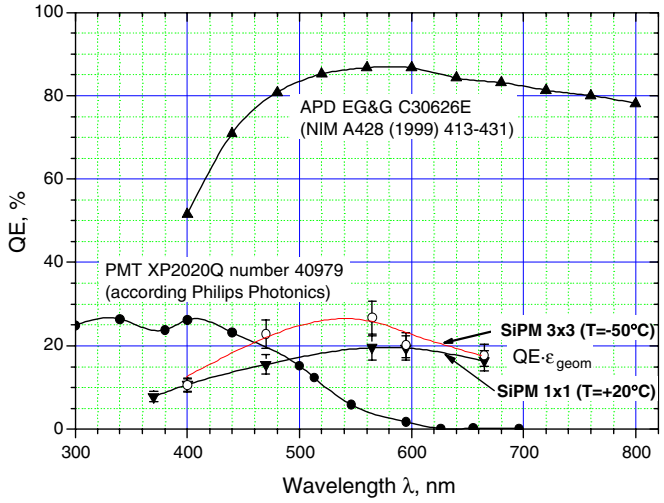

Fig. 1. Comparison of the photon detection efficiency for SiPM, APD and PMT.

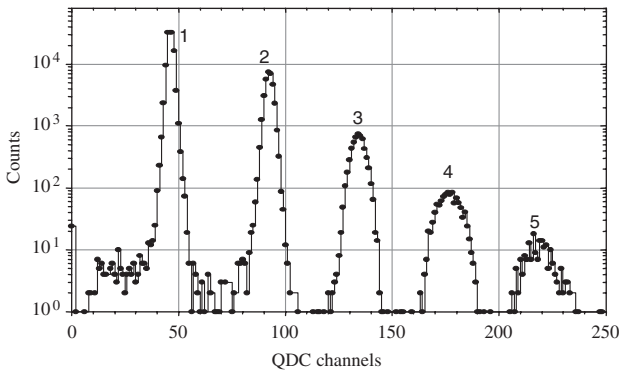

Fig. 2. Dark rate pulse height distribution.

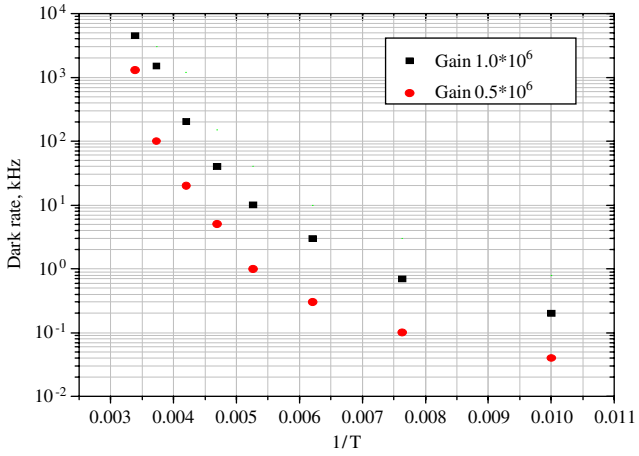

Fig. 3. Temperature dependence of the SiPM dark rate for different one pixel gains.

- a very low excess noise factor (ENF) for each single pixel due to the Geiger mode operation, in contrast the large ENF for APDs due to fluctuations in the avalanche development process.

The single photoelectron (single pixel) resolution is important for calibration and monitoring, because it allows to directly measure the SiPM gain via the distance between the maxima of pulse hight distribution.

1.5. Single pixel dark rate

The electronics noise of SiPMs is negligibly small due to the very high gain (~10^6), in contrast to standard APDs, where the gain is typically about 100. In SiPM, the level of electronics noise corresponds to less than 10% of the signal from one photoelectron.

The main source of noise, which limits the SiPM's single photon resolution is the dark rate, originating from charge carriers thermally created in the sensitive volume. The SiPM dark rate decreases with temperature from a few (typically 1–2) MHz/mm^2 (room temperature) to ~200 Hz/mm^2 (at 100 K)—see Fig. 3.

For the detection of very small light signals (one or a few photoelectrons) on larger sensitive area this dark rate limits the SiPM performance at room temperatures. The rate can be reduced by operating at lower temperature, and by improving the SiPM production technology. The detection of large light signals is practically unaffected.

1.6. Inter-pixel crosstalk

The SiPM pixels should be decoupled from each other and work as independent photon micro-counters. Electrical decoupling is realized by

- polysilicon quenching resistors for each pixel, which limit the Geiger discharge and at the same time electrically decouple pixel from pixel,
- specially designed boundaries between pixels in order to inhibit inter-pixel currents in the silicon itself. These boundaries occupy part of the SiPM surface and reduce the sensitive area (geometrical efficiency).

Another type of inter-pixel coupling is introduced by "optical crosstalk". It originates from photons created in the Geiger discharge with a rate of about 10^{-5} photons per electron [8]. These photons can propagate to another not primarily fired pixel and initiate a discharge there. Optical crosstalk violates the pixel independence and leads to a non-Poissonian behavior of the distribution of the number of fired pixels. In Fig. 2, showing the dark rate pulse height distribution, one can see a long non-Poissonian tail, indicating an increased probability of multi-pixel firing.

For low dark rates (dark rate × SiPM pulse width $\ll 1$) an optical crosstalk coefficient $K_{2/1}$ can be defined as the probability for a second pixel to be fired. This coefficient (see Fig. 4) rises with the SiPM gain, since the number of secondary photons increases. The figure of merit is here the dark rate above a certain threshold. The dark rate dependence on gain, or bias voltage, is shown in Fig. 5. The requirement to have a sufficiently low dark rate limits the gain for current SiPM's at the level of 10^6, and the PDE to 10–15% (at room temperature).

1.7. The timing by SiPM

The SiPM response is intrinsically very fast (less than 500 ps) due to the very thin depletion layer and the extremely short duration of the Geiger discharge development.

The single photoelectron timing resolution is characterized by $\mathrm{FWHM}_0 = 100$ ps ([2,3]) for photons absorbed in the depletion region. The dependence of the timing resolution on $N_{\mathrm{photoelectrons}}$ through $\mathrm{FWHM} = \mathrm{FWHM}_0/(N_{\mathrm{photoelectrons}})^{1/2}$ has been shown to be valid up to $N_{\mathrm{photoelectrons}}$ of 100. It should be noted that such a single photoelectron timing resolution can be achieved using just a leading edge discriminator because the single photoelectron (single pixel) pulse is very stable (see Fig. 2).

The excellent timing properties of the SiPM can be useful for matching of the scintillation tile calorimeter signals in time to the bunch crossing of the collider with a resolution of about 1 ns, which is determined by the rise time of scintillator + WLS fiber signal [9]. In the core of electromagnetic showers, with a signal corresponding to about 40 MIPs, a timing resolution of ~200 ps can be obtained.

The time for each pixel to recover from the discharge is also small. It is determined by the product of pixel capacity and polysilicon resistance, $\tau_R = C_{\mathrm{pixel}} R_{\mathrm{Si}}$. For polysilicon resistor values of 0.5–5 MΩ the recovery time of one pixel ranges between 25 and 250 ns.

1.8. SiPM dynamic range

The finite number of SiPM pixels determines the dynamic range of the SiPM, and it leads to a nonlinearity

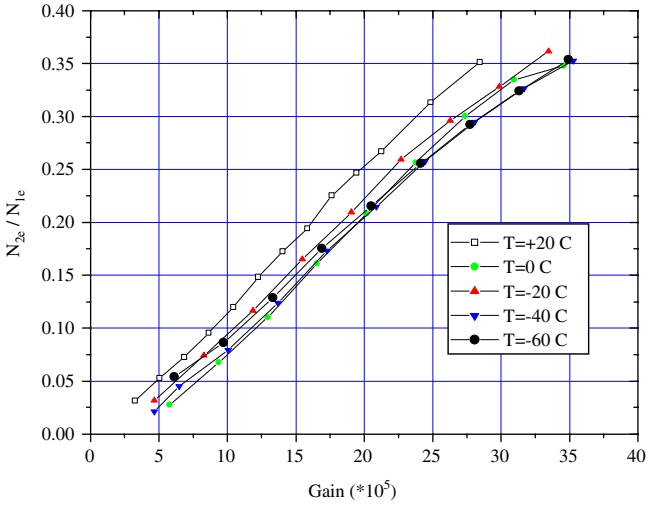

Fig. 4. Optical crosstalk coefficient (probability for second pixel to be fired compared a single pixel rate) vs SiPM one pixel gain.

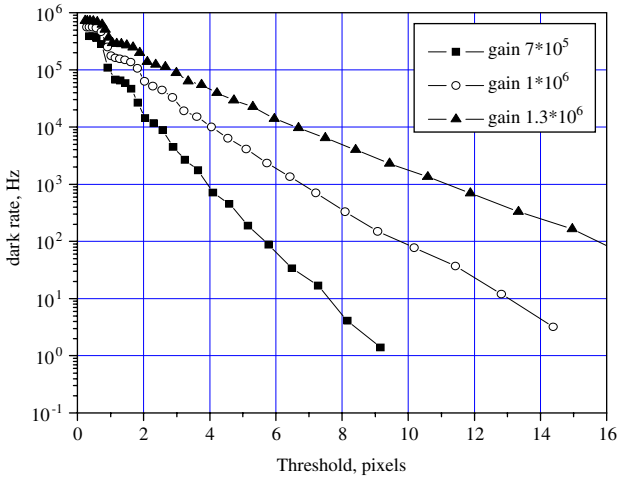

Fig. 5. Dark rate of the SiPM for different gains in dependence on the level of the threshold.

of the SiPM response when the number of produced photoelectrons approaches the total number of pixels. Saturation occurs if the number of photoelectrons per pixel ~1. However, this is valid only if the duration of the light signal Δt is much smaller than the single pixel recovery time τ_R. For long enough light signals ($\Delta t > \tau_R$) the SiPM dynamic range is larger.

On the other hand, in such a situation the nonlinear response function is strongly dependent on the width of the light pulse (see Fig. 6), which can complicate the nonlinearity correction procedure. A recovery time large compared to the light pulse duration would eliminate this potential problem; this would require the choice of a larger value for the polysilicon resistor.

1.9. SiPM sensitivity to temperature and bias voltage

The SiPM response to a given light signal depends on the product of PDE and single pixel gain. Both factors depend on the overvoltage $\Delta V(T) = V_{\text{bias}} - V_{\text{breackdown}}(T)$ and thus on the supplied bias voltage and via $V_{\text{breackdown}}$ also on the temperature T. The gain variation is 1.7%/°C and 2.5%/0.1 V, and the overall SiPM signal amplitude variation is 4.5%/°C and 7%/0.1 V for a SiPM gain of 10^6. The sensitivity to temperature and bias voltage decreases with increasing gain (and overvoltage).

1.10. Calibration and monitoring of SiPMs

The stability of the response of an individual scintillator + SiPM element can be monitored by using the position of the MIP or an α-source signal. Fig. 7 demonstrates the possibility of such a monitoring concept for a 50 mm × 50 mm × 5 mm scintillator tile + WLS + SiPM system. It shows the single pixel spectrum obtained by using an LED, the MIP signal (here from a Sr^{90} β source) and the signal generated by a Pu^{238} α-source. Because the plastic scintillator itself has very low light yield for α-particles, a very small (5 mm × 5 mm × 70 μm) YAP scintillator crystal has been glued on the centre of the plastic scintillator tile. The clear separation of the SiPM signal generated by a single particle provides a direct determination of the energy scale

$$\frac{\text{energy deposition by MIP}}{\text{number of pixels fired}}$$

for each scintillator element. The response measured in number of pixels per MIP must be known for corrections of the non-linear SiPM behavior, since the SiPM dynamic range is determined by the total number of pixels.

As already mentioned, the resolution of single pixel signals offers a unique possibility to perform a direct and absolute measurement of the SiPM gain and thus to monitor each SiPM for possible corrections due to variation of the temperature and bias voltage with time ("auto-calibration"). Using the known characteristics of the SiPM, the expected change in total response can be inferred from the observed change in gain. Direct gain measurement and radioactive sources thus provide alternatives to the more conventional method using a stabilized light source as reference signal.

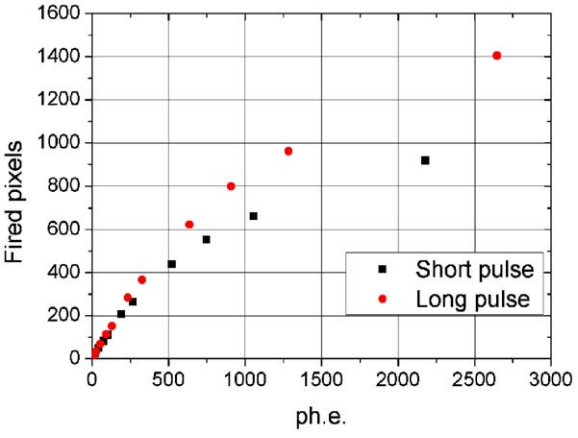

Fig. 6. Nonlinear response to LED light signals with different pulse durations.

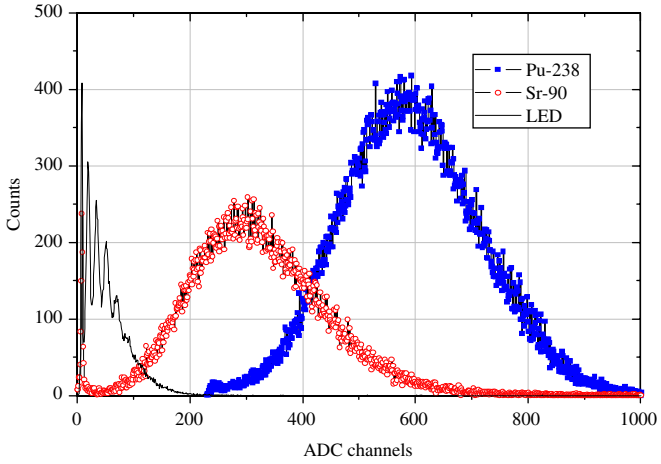

Fig. 7. SiPM spectra for LED, β-particles from Sr^{90} and α-particles from Pu^{238} source.

1.11. Low bias voltage, low power consumption

The breakdown electric field in Si is about 2.5×10^5 V/cm. Since the SiPM depletion zone is typically 1–3 μm thin, the working bias voltage is rather low (25–75 V). This is comfortable for the design of systems with a large number of SiPM's. For instance, a single coax cable is needed to supply bias voltage and provide the signal line to one SiPM, and one can even use the cable screen as bias voltage line.

The typical dark current for a 1 mm^2 SiPM is about 1 μA. Therefore the corresponding power consumption is also very small (~50 μW).

1.12. SiPM compactness

The SiPM device is very compact: for 1 mm × 1 mm sensitive area the total SiPM size is as small as 1.5 mm × 1.5 mm with a thickness of 300 μm of Si. Together with the low bias voltage and power consumption, this opens up new possibilities for the readout of scintillator elements: to mount the SiPM directly embedding the photodetector into the body of the scintillator (see Fig. 8).

1.13. SiPM: very low charge particle sensitivity (negligible nuclear counting effect)

The SiPM signal does not depend on the number of primary carriers created (because of the Geiger mode operation). Thus, each pixel detects the carriers created by a photon, by a minimum ionizing particle, or by thermal excitation with the same response signal of $\sim 10^6$ electrons. Together with the compactness, this implies that the nuclear counter effect is negligible for SiPMs, and they can be located inside the calorimeter, for example.

1.14. Insensitivity to magnetic field

Most calorimeters for collider detectors operate in high magnetic fields. The operation of SiPMs has been tested in a magnetic field up to 4 T for two orientations of the field lines [10] and it was shown that the SiPM signal is stable within 1% measurement accuracy. Furthermore, dark current, noise frequency, gain and pixel crosstalk of SiPM have been measured at 4 T and found to be magnetic field independent.

1.15. Large area SiPM's [11]

There are some limitations for the performance of large area, high gain and high PDE SiPMs:

- the dark rate, which increases proportionally with area,
- power dissipation,
- optical crosstalk.

All these reasons are more and more significant for larger area SiPM with high packing efficiency of the pixels and limit the SiPM size at the level of $\sim 10 \times 10\,\mathrm{mm}^2$ for moderate cooling (−30 to −50 °C). Nevertheless, the SiPM with area of $3 \times 3\,\mathrm{mm}^2$ has been successfully built and operated [11]—see Figs. 9 and 1, where its PDE is shown.

1.16. SiPM long term stability and ageing

Two dedicated tests have been performed in order to study the SiPM long-term stability and ageing under different conditions.

First, a sample consisting of 20 SiPMs (1 mm × 1 mm, 576 pixels) was operated under bias voltage corresponding to a gain of 1×10^6 during 1500 h at room temperature. The SiPM parameters such as gain, PDE, dark noise rate and dark current were measured before the test, after 500 and 1500 h of operation.

Second, possible ageing of 5 SiPMs with 1024 pixels was studied under extreme temperature conditions ranging from room temperature up to 90 °C, increased in steps of 10 °C. At each temperature point the SiPMs were operated for 24 h with a gain of 1×10^6 (with increasing temperature the bias voltage was increased, too). The SiPM parameters did not show any variation during these stability tests. More long-term SiPM stability studies including the radiation resistance are needed and planed in nearest future.

2. Some examples of SiPM applications

2.1. Scintillator+WLS+SiPM systems

2.1.1. High-granularity Sci Tile Hadron Calorimeter prototypes for International Linear e^+e^- Collider Detector [10,12,13]

The precision physics program at a future Linear Collider (LC) requires reconstructing hadronic final states of heavy boson (W, Z, H) decays in multi-jet events. For this purpose a jet energy resolution of better than $30\%/\sqrt{E}$ is necessary. Monte Carlo simulations demonstrate that such a resolution can be achieved using a novel "particle flow" approach in which each particle in a jet is measured

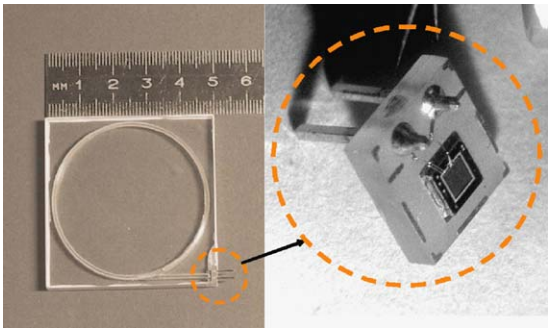

Fig. 8. SiPM mounted directly on tile.

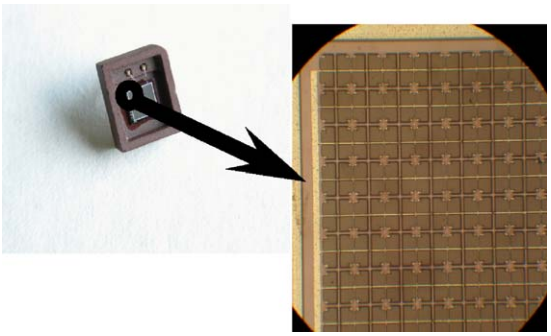

Fig. 9. SiPM $3 \times 3\,\mathrm{mm}^2$, 5625 pixels.

individually. In this approach the calorimeter must have very fine longitudinal and transverse segmentation. For hadron shower separation a transversal segmentation of about $3 \times 3\,cm^2$ is needed, and every sampling layer should be read out individually. Such a granularity can be realized on large scale using scintillator tiles with wave length shifter (WLS) fiber light collection, individually read out by SiPM)as photodetectors.

A first prototype calorimeter based on scintillator tiles of $5\,cm \times 5\,cm \times 5\,mm$ size (Fig. 8) with 108 channels ("minical") has been constructed. The light yield of the tiles produced a signal corresponding to 25 ± 4 fired pixels per MIP. The calorimeter design, data taking, calibration and results are reported in Ref. [10].

This "minical" has been successfully operated in the DESY positron test beam at energies of from 1 to 6 GeV. Nonlinearity effects due to the limited number of pixels were noticeable in the shower core; for 6 GeV electromagnetic showers the energy depositions were ranging up to an equivalent of 70 MIPs per tile). The effects could successfully be corrected for each channel using the well-measured SiPM response function. Fig. 10 shows the measured energy resolution as a function of beam energy. The data compare well with results obtained with conventional multi-anode vacuum phototubes and they are well reproduced by a Monte Carlo simulation, which includes the detailed SiPM behavior. This leads to conclusion that after correction the saturation effects do not degrade the calorimeter linearity and resolution.

The next step in the development of a high granularity scintillator tile hadron calorimeter is the $1\,m^3$ prototype [12,13] which is being constructed by the CALICE collaboration and consists of 40 layers of 3×3, 6×6 and $12 \times 12\,cm^2$ 0.5 cm thick tiles + WLS fibers + -SiPMs. Fig. 11 shows one layer of this prototype under assembly. The total number of channels is 8000 and requires a significant advancement in mass production and quality control.

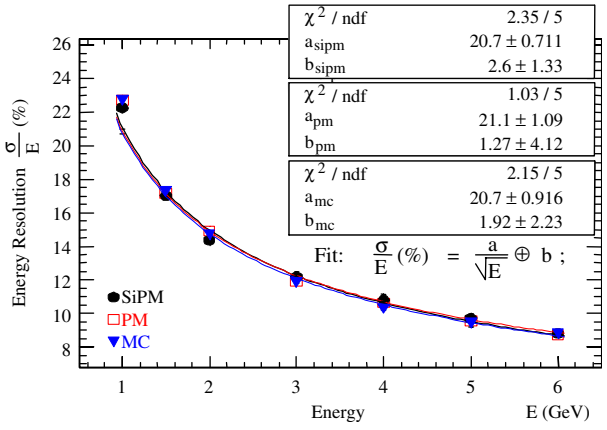

Fig. 10. Measured energy resolution for SiPM with (solid points), MAPM (squares) and MC prediction (triangles).

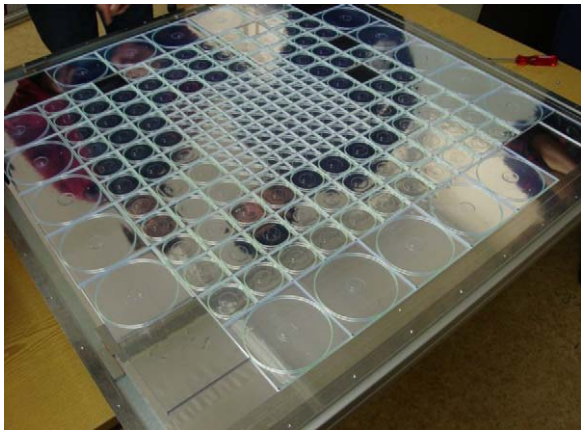

Fig. 11. One plane with SiPMs and WLS fibers installed into 3×3, 6×6 and $12 \times 12\,cm^2$ 0.5 cm thick tiles.

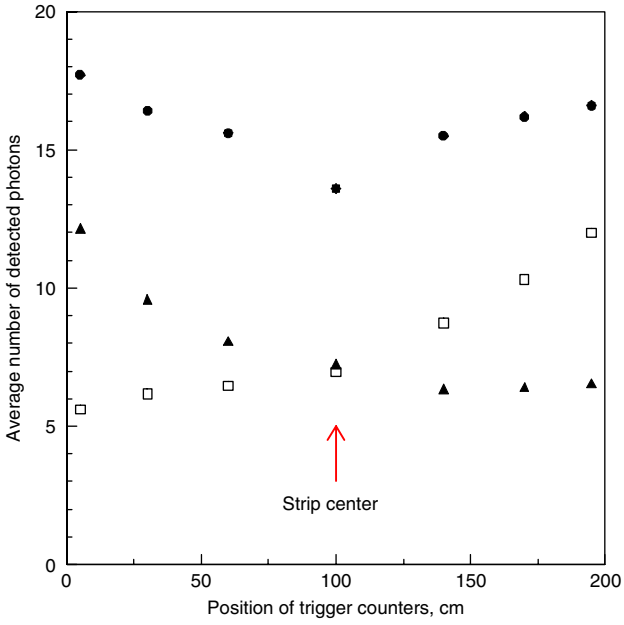

Fig. 12. SiPM pulse height in number of photoelectrons vs MIP particle coordinate along the scintillation bar (2.5 cm × 1 cm × 2 m). Lower curves correspond the individual SiPM from both ends of the bar, upper one is a sum of both SiPM's.

2.1.2. Scintillator-based hodoscope with SiPMs

Fig. 12 shows an example of such a scintillator + WLS + SiPM system for $2\,m \times 25\,mm \times 10\,mm$ rod [14]: an efficiency for MIP detection of more than 99% has been achieved even with a SiPM on one end only.

A ($5\,cm \times 5\,cm \times 5\,mm$) hodoscope scintillator tile + WLS + SiPM prepared by MEPHI-ITEP has been successfully operated within the space experiment LAZ10 (MEPHI-INFN collaboration) on the International Space Station (launched on 15 April 2005) for the measurement of low-energy particle fluxes and radiation monitoring. Fig. 13 displays the latitude particle flux dependence measured by this space SiPM based hodoscope.

Another example of such a hodoscope is the $8\,m^2$ Alice TOF Cosmic Test System [15] with scintillator tiles of

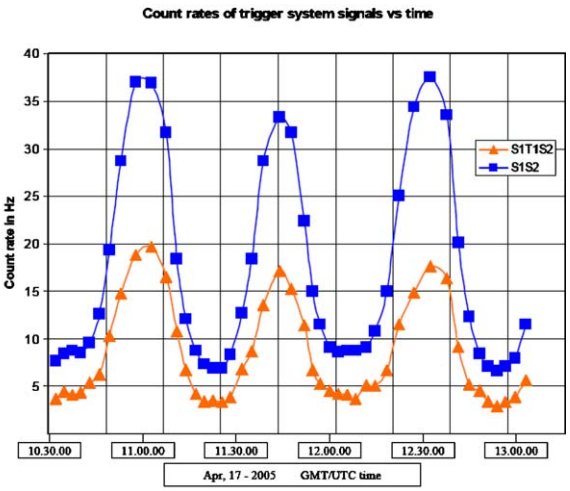

Fig. 13. Sci + WLS fiber + SiPM hodoscope system in space experiment LAZ10.

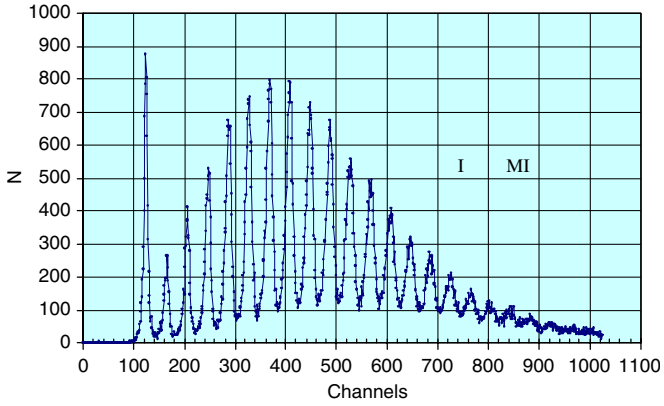

Fig. 14. MIP detection by sci fiber + SiPM.

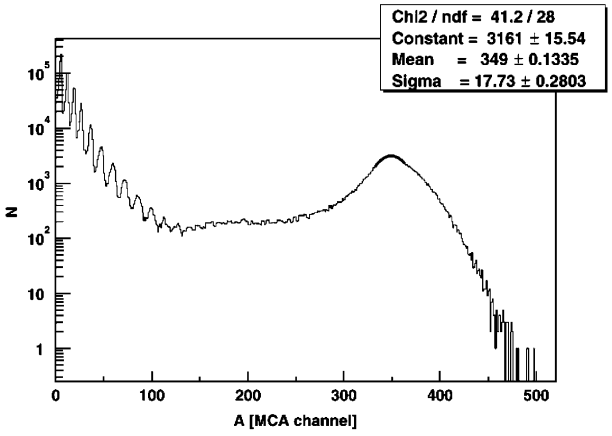

Fig. 15. Am ^{241} α-particle scintillations in LXe, 178 nm, −95 °C).

$15 \times 15 \times 1\,cm^3$ size.[1] A timing resolution of ~1.2 ns has been obtained.

2.2. SiPM application for scintillating fiber MIP detection

Fig. 14 shows the pulse height spectrum from MIP detection by (Kuraray SCSF-78 M) 1 mm diameter scintillating fiber + SiPM at room temperature. One can see the Landau-like distribution with clearly separated photoelectron (fired pixel) peaks (~9 pixels/MIP).

2.3. SiPM usage for liquid Xe scintillation detection

This application confirms the possibility of vacuum UV light detection by SiPMs in experiments on dark matter WIMPS search [16]. The scintillation light in liquid Xe (−95 °C) has a wavelength of 178 nm, The pulse hight spectrum of Am^{241} α particles is shown in Fig. 15; a PDE of the SiPM (1 mm × 1 mm, 576 pixels) of 5.5% for $\lambda =$ 178 nm has been measured.

2.4. A few examples of larger area ($3 \times 3\,mm^2$) SiPMs applications

2.4.1. Transition X-ray detection

Transition Radiation X-ray detectors based on very thin heavy scintillator + SiPM appear to be more robust and fast than traditional Xe gas based TRDs, especially for space physics applications (no gas, no high voltage). Fig. 16 shows the results from a test prototype [11] based on $3 \times 3\,mm^2$ SiPM + 70 μm YAP:Ce crystal. Such a system is a promising candidate for a base element of multiset TR detectors.

2.4.2. Time-of-flight measurements with SiPM [9,11]

The timing resolution of a system consisting of a 3×3 mm^2 SiPM + plastic scintillator BC418 ($3 \times 3 \times 40\,mm^3$,

[1]This hodoscope used the Geiger mode APD called MRS APD (which is quite similar to SiPM), produced by the Centre of Perspective Technology and Apparatus, Moscow.

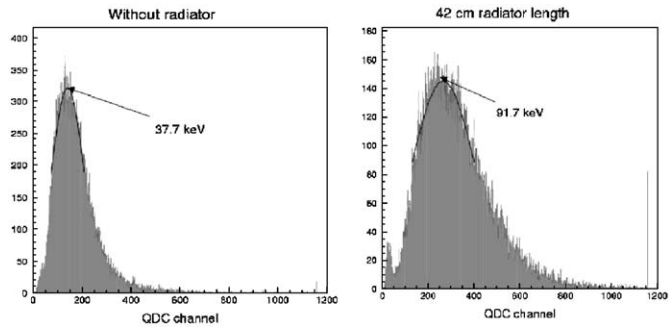

Fig. 16. Pulse height distributions for TR X-ray detection with one polypropylen foils radiator and YAP:Ce crystal + $3 \times 3\,mm^2$ SiPM.

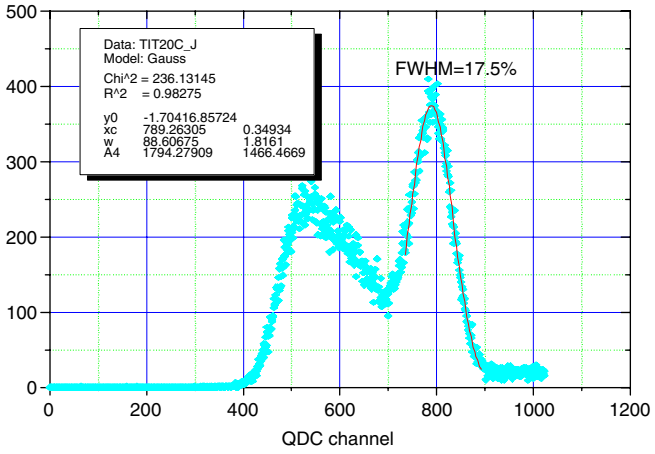

Fig. 17. Pulse height distribution for 511 keV gamma's, obtained by LYSO ($3 \times 3 \times 20\,mm^3$) + $3 \times 3\,mm^2$ SiPM system.

decay time 1.4 ns) has been measured for 3 GeV electrons, σ(SiPM + BC418) = 32 ps. Such a result confirms the high potential of TOF systems based on large-area SiPM + plastic scintillator elements.

2.4.3. SiPM application for Positron Emission Tomography (PET)

Fig. 17 demonstrates the possibility for detection of PET photons (511 keV) by an SiPM ($3 \times 3\,mm^2$) coupled to a LYSO crystal ($3 \times 3 \times 20\,mm^3$). A pulse height resolution of 17.5% (FWHM) and a timing resolution between two PET photons of 780 ps have been measured [9,11]. Low power consumption, low voltage, excellent timing and compactness give rise to a high potential for SiPMs to be used for new generation of PET tomographs [11,17].

3. Conclusions

The Silicon Photomultiplier is becoming a photodetection device competitive to PMT and APD for a number of applications. A new generation of SiPMs with reduced

- optical crosstalk,
- dark rate,
- afterpulsing (due to trap and delayed release of electrons in a Geiger discharge),

is under development now in order to obtain SiPMs with

- area up to $10 \times 10\,mm^2$,
- photon detection efficiency of 40–50%,
- excess noise factor as low as a few %,
- subnanosecond timing.

It will significantly increase the number of SiPM applications even further.

References

[1] G. Bondarenko, B. Dolgoshein, V. Golovin, A. Ilyin, R. Klanner, E. Popova, Nucl. Phys. B (Proc. Suppl.) 61B (1998) 347 and reference therein;
G. Bondarenko, P. Buzhan, B. Dolgoshein, V. Golovin, E. Guschin, A. Ilyin, V. Kaplin, A. Karakash, R. Klanner, V. Pokachalov, E. Popova, K. Smirnov, Nucl. Instr. and Meth. A 442 (2000) 187 and references therein.

[2] P. Buzhan, B. Dolgoshein, L. Filatov, A. Ilyin, V. Kantzerov, V. Kaplin, A. Karakash, F. Kayumov, S. Klemin, A. Pleshko, E. Popova, S. Smirnov, Yu. Volkov, The advanced study of silicon photomultiplier, in: Proceedings of the Seventh International Conference on Advance Technology & Particle Physics, 2002, pp. 717–728.

[3] P. Buzhan, B. Dolgoshein, L. Filatov, A. Ilyin, V. Kantzerov, V. Kaplin, A. Karakash, F.P. Buzhan, B. Dolgoshein, L. Filatov, A. Ilyin, V. Kantzerov, V. Kaplin, A. Karakash, F. Kayumov, S. Klemin, E. Popova, S. Smirnov, Nucl. Instr. and Meth. A 504 (2003) 48.

[4] B. Dolgoshein (on behalf of SiPM-Collaboration), Silicon Photomultipliers in particle physics: possibilities and limitations, presented at Workshop "Innovative Detectors for Future Colliders", Erice, Italy, October. 2003.

[5] D. Renker, Talk given at Beaune-2005 Conference and references therein, in: Proceedings of Fourth International Conference "New Development in Photodetection", June 2005, Beaune, Nucl. Instr. and Meth. A, submitted for publication.

[6] Yu. Musienko, Contribution given at Beaune-2005 Conference, in: Proceedings of Fourth International Conference "New Development in Photodetection", June 2005, Beaune, Nucl. Instr. and Meth. A, submitted for publication.

[7] Z. Sadygov, Talk given at Beaune-2005 Conference and references therein, in: Proceedings of Fourth International Conference "New Development in Photodetection", June 2005, Beaune, Nucl. Instr. and Meth. A, submitted for publication.

[8] P. Lacaita, F. Zappa, S. Bigliardi, M. Manfredi, IEEE Trans. Electron Dev. 40 (3) (1993) 577.

[9] Karakash, Contribution given at Beaune-2005 Conference, in: Proceedings of Fourth International Conference "New Development in Photodetection", June 2005, Beaune, Nucl. Instr. and Meth. A, submitted for publication.

[10] V. Andreev, V. Balagura, B. Bobchenko, P. Buzhan, J. Cvach, M. Danilov, et al., Nucl. Instr. and Meth. A A540 (2005) 368.

[11] Dolgoshein, Talk given at Beaune-2005 Conference, in: Proceedings of Fourth International Conference "New Development in Photodetection", June 2005, Beaune, Nucl. Instr. and Meth. A, submitted for publication.

[12] M. Danilov, Talk given at Lepton-Photon Simposium, 2005;
F. Sefkow, in: proceedings of LCWS2005, Stanford, USA, 2005.

[13] E. Popova, Talk given at Beaune-2005 Conference, in: Proceedings of Fourth International Conference "New Development in Photodetection", June 2005, Beaune, Nucl. Instr. and Meth. A, submitted for publication.

[14] V. Balagura, et al., Study of Scintillator Strip with Wavelength Shifting Fiber and Silicon Photomultiplier, Nucl. Instr. and Meth. A, submitted for publication.
[15] Martemyanov, Talk given at Beaune-2005 Conference, Proceedings of Fourth International Conference "New Development in Photo-detection", June 2005, Beaune, Nucl. Instr. and Meth. A, submitted for publication.
[16] E. Aprile, P. Cushman, K. Nu, P. Shagin, Nucl. Instr. and Meth. A, submitted for publication.
[17] A.N. Otte, et al., Nucl. Instr. and Meth. A 545 (2005) 705.